The Canadian Mineralogist
Vol. 42, pp. 1357-1368 (2004)

EXPERIMENTAL SIMULATION OF SHOCK-INDUCED RE-EQUILIBRATION OF FLUID INCLUSIONS

MEGAN E. ELWOOD MADDEN[§]

Department of Geosciences, Virginia Tech, 4044 Derring Hall, Blacksburg, Virginia 24061, U.S.A.

FRIEDRICH HORZ

Astromaterials Research Office, Mailcode SR, NASA Johnson Space Center, Houston, Texas 77058, U.S.A.

ROBERT J. BODNAR[§]

Department of Geosciences, Virginia Tech, 4044 Derring Hall, Blacksburg, Virginia 24061, U.S.A.

ABSTRACT

Meteorite impacts and their attendant shock waves create conditions of extremely high strain-rates, temperatures, and pressures. As the role of fluids in our Solar System becomes increasingly recognized and studied, it is important to understand the effects of shock on fluid-bearing materials. In this study, the effects of 5–30 GPa experimental shock waves on aqueous fluid inclusions in single-crystal quartz were observed and quantified. The homogenization temperatures of fluid inclusions within the samples and other physical features were documented before and after the experimental shock events. The properties of fluid inclusions show a systematic and gradual evolution with increasing shock pressure. Some fluid inclusions survive shock pressures of 6 GPa, yet they exhibit an increase in homogenization temperature relative to pre-impact measurements, suggesting that re-equilibration occurred because of internal overpressures. Decrepitated fluid inclusions were observed in the 6 and 7.6 GPa samples, whereas textures indicative of the collapse of fluid inclusions due to internal underpressure were observed in samples shocked at 7.6–12 GPa. No features that could be directly related to fluid inclusions were observed in samples shocked at pressures greater than 12 GPa. Results of these experiments suggest that fluid inclusions initially undergo a decrease in volume during shock compression. If the fluid inclusions survive this event, the initial decrease in volume is overprinted by the subsequent effects of elevated temperature at ambient pressure, leading to an increase in inclusion volume and homogenization temperature. Therefore, homogenization temperatures of fluid inclusions found in shocked materials should be considered a maximum value, as the density of the originally trapped fluid was likely greater than that observed in shock-processed inclusions. These results suggest that the rarity of fluid inclusions in meteorites may be a result of shock processing, and may not reflect a fluid-poor environment on the parent body.

Keywords: fluid inclusions, quartz, re-equilibration, experimental impacts, shock metamorphism, meteorites.

SOMMAIRE

Les impacts météoritiques et les ondes de choc qui en résultent créent des conditions favorisant des taux de déformation, des températures et des pressions extrêmement élevés. A mesure que le rôle des phases fluides dans notre système solaire attire de plus en plus d'attention, il est essentiel de bien comprendre les effets des ondes de choc sur les matériaux à composantes fluides. Ce travail porte sur les effects d'une onde de choc d'entre 5 et 30 GPa générée expérimentalement sur les inclusions fluides aqueuses piégées dans des monocristaux de quartz. La température d'homogénéisation de ces inclusions et d'autres caractéristiques physiques ont été documentées avant et après l'événement de choc. Les propriétés des inclusions fluides montrent une évolution graduelle et systématique à mesure qu'augmente l'intensité de l'onde de choc. Certaines inclusions survivent à une pression de choc de 6 GPa, mais elles montrent une augmentation de la température d'homogénéisation par rapport aux inclusions avant l'impact, ce qui indique un ré-équilibrage à cause d'une surpression interne. Nous avons remarqué des inclusions fluides décrépitées à 6 et à 7.6 GPa, tandis que les textures indicatives d'un affaissement des inclusions fluides à cause du développement d'un vide de décompression ont été observées dans les échantillons dont l'onde de choc faisait entre 7.6 et 12 GPa. Nous ne voyons aucun signe de la présence d'inclusions fluides dans les échantillons sujets à une pression transitoire dépassant 12 GPa. Les résultats de ces expériences font penser que les inclusions fluides subissent d'abord une diminution en volume due à la décompression transitoire. Si elles survivent à ce stade, cette diminution initiale est renversée à cause des effets d'une température

§ *E-mail addresses*: melwood@vt.edu, rjb@vt.edu

élevée à pression ambiante, ce qui mène à une augmentation du volume et de la température d'homogénéisation. C'est donc dire que la température d'homogénéisation des inclusions fluides dans les matériaux ayant subi un métamorphisme de choc aurait une valeur maximale, parce que la densité de la phase fluide piégée à l'origine était probablement supérieure à celle qui est observée dans les inclusions ayant subi un choc. D'après ces résultats, il semble que la rareté des inclusions fluides dans les météorites pourrait résulter d'un remaniage dû au choc, et non de l'absence relative de fluides dans le milieu de formation de la météorite.

(Traduit par la Rédaction)

Mots-clés: inclusions fluides, quartz, ré-équilibrage, impacts expérimentaux, métamorphisme dû à un impact, météorites.

Introduction

Fluid inclusions in terrestrial rocks are the rule rather than the exception, but only a few fluid-inclusion-bearing meteorites have been documented (Bodnar 1999, Zolensky *et al.* 1999, Bridges & Grady 2000, Rubin *et al.* 2002). The rarity of fluid inclusions in meteoritic materials may be explained in two ways: first, it may reflect the absence of fluids on meteorite parent bodies. However, significant features involving aqueous alteration and phases observed in many apparently fluid-inclusion-free meteorites suggest that fluids were present on their parent bodies (Zolensky & McSween 1988, Bischoff 1998, Bridges *et al.* 2001), contradicting this hypothesis. Alternatively, fluid inclusions originally trapped on the parent body may have been destroyed by the extreme P–T conditions that meteorites experience during impact events. Just as textures, structures, and compositions of mineral phases can be significantly altered by shock waves, fluid inclusions contained within component minerals may be altered or destroyed owing to the high pressures, temperatures, and strain rates associated with collisional events. As interest in the occurrence of H_2O in our Solar System grows, it is important to develop additional tools that can be used to test for the presence of H_2O in present or past planetary environments. Fluid inclusions in meteorites and other impact-related samples provide one such tool, and it is thus important to understand shock metamorphism of fluid-bearing materials. In this study, we test the effects of experimental impacts on fluid inclusions trapped in single-crystal quartz to better understand the pressure – temperature – time (P–T–t) path that fluid inclusions and their host minerals experience during shock events. These data can be applied to fluid inclusions in shocked meteorites as well as terrestrial rocks and may lead to a better understanding of why fluid inclusions are so rare in meteorites. In addition, the experimental results help to constrain P–T–t conditions during impact events, especially at low pressures, and they may serve to reconstruct the pre-impact fluid conditions in shocked materials.

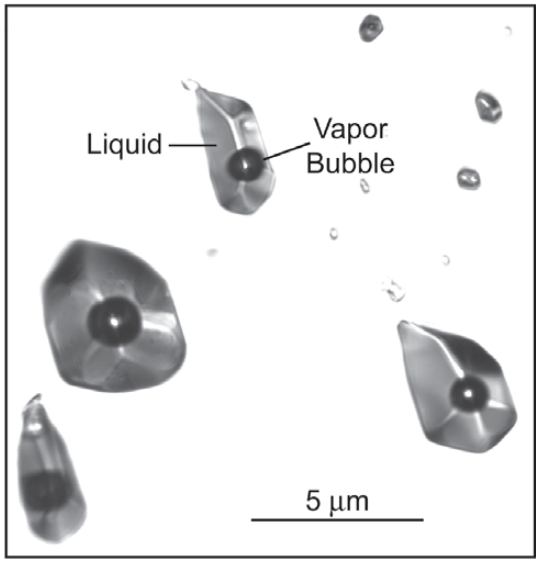

FIG. 1. Photomicrograph of two-phase fluid inclusions in Arkansas quartz. Euhedral fluid inclusions of various sizes maintain the negative-crystal shape of the quartz host. All fluid inclusions in the figure contain a liquid phase (water) and a bubble containing water vapor at room temperature. As the sample is heated, the density of the liquid phase decreases, and the vapor bubble shrinks until the homogenization temperature (T_h) is reached (see Fig. 2), at which point the vapor bubble disappears and the inclusion is filled with one homogeneous fluid phase. The homogenization temperature is directly related to the density of the trapped fluid, therefore providing information on the P–T conditions under which the fluid was trapped.

Background Information

Fluid inclusions are micrometer- to millimeter-sized samples of fluid (H_2O, CO_2, igneous melt, *etc.*) trapped within minerals as they precipitate in the presence of that fluid phase (Fig. 1). Fluid inclusions are nearly ubiquitous in terrestrial minerals formed in the presence of a fluid. Conversely, fluid inclusions in extraterrestrial materials are relatively rare, although fluid inclusions have been documented in both chondritic and achondritic meteorites. Fluid inclusions observed in the Monahans (1998) and Zag H5 chondrites are believed to have formed during alteration of the parent body, shortly after its formation in the early Solar System

(Zolensky *et al*. 1999, Rubin *et al*. 2002). Fluid inclusions in SNC meteorites (Shergotty – Nakhla – Chassigny type, originating on Mars), such as the CO_2 inclusions found in Nakhla and ALH84001 (Bodnar 1999), provide evidence of *in situ* processes involving fluids on Mars. These samples of fluid, trapped during mineral growth in the Martian mantle, provide evidence that may be used to decipher the early magmatic history of Mars and the source of volatiles in its early oceans and atmosphere. Whereas these occurrences of fluid inclusions in meteorites are extremely rare, they offer important and unique opportunities to constrain pressure–temperature conditions and fluid compositions during the formation and alteration of parent bodies of the meteorite. Therefore, it is imperative that we understand why fluid inclusions are so rare in meteoritic materials, whether it be a result of a lack of fluids on the parent bodies or subsequent alteration and processing of meteoritic material, to better characterize the role of fluids throughout the Solar System and to direct our search for evidence of fluids and fluid inclusions in meteorites.

Meteorites may experience extreme conditions of pressure and temperature during the evolution of their parent bodies and in the process of being ejected from their parent bodies and upon arrival on Earth. Most SNC meteorites show evidence of impact pressures up to, and in some cases exceeding, 40 GPa (Stoffler *et al*. 1986, Greshake 1998, Langenhorst & Greshake 1999, El Goresy *et al*. 2000, Malavergne *et al*. 2001, Fritz *et al.* 2003). Impact textures and phases observed in chondritic meteorites indicate shock pressures ranging from negligible levels to melting at >60 GPa (Stoffler *et al.* 1991, Schmitt & Stoffler 1995, Rubin *et al.* 1997; note that higher shock pressures associated with melting and vaporization are possible, but here we limit the discussion to "solid state" deformation). Fluid inclusions interpreted as having been formed pre-impact have also been documented in terrestrial impact sites (Koeberl *et al.* 1989). Impact events subject material not only to extremely high strain-rates and pressures, but also to elevated temperatures (Langenhorst 1994). These high-temperature, high-pressure conditions may lead to re-equilibration (change in fluid density) of any fluid inclusion that might be contained in shocked materials, as suggested by Komor *et al.* (1988) in a study of fluid inclusions in the Siljan Ring impact structure. Complete collapse and physical destruction of fluid inclusions seem possible as well and may explain the relative scarcity of fluid inclusions in meteorites.

Re-equilibration of fluid inclusions may occur when the external pressure on the sample and the internal pressure in the fluid inclusion differ. "Re-equilibration" is a general term that refers to any change that an inclusion may undergo following formation, including a change in volume or shape, or the loss or gain of fluid along fractures or by diffusion through the host crystal (Vityk *et al.* 2000; their Fig. 1; Bodnar 2003). For quartz, the mineral that is the focus of this investigation, fluid inclusions will generally begin to re-equilibrate if the pressure difference exceeds about 0.2 GPa (Bodnar *et al.* 1989, Vityk *et al.* 1994). The magnitude of the difference required to re-equilibrate fluid inclusions varies as a function of the strength and cleavage of the host mineral, as well as the size and shape of the inclusions and the absolute distance of inclusions from free surfaces, such as fractures, cleavage planes and mineral surfaces (Tugarinov & Naumov 1970, Ulrich & Bodnar 1988, Bodnar *et al*. 1989). The likelihood that re-equilibration will occur can be predicted by comparing the external pressure conditions applied on the host mineral to the pressure conditions within the fluid inclusion at any point on the P–T–t path. Whereas the external pressure exerted on the host mineral is dependent on the load applied, the pressure inside the fluid inclusion is controlled by the isochore (line of constant density) for the fluid. Therefore, the temperature of the rock and the PVT properties of the fluid determine the internal pressure of the inclusion.

At any temperature, the internal pressure of a fluid inclusion trapped at T_t, P_t (point A, Fig. 2) is constrained by the isochore that extends from the conditions of formation (point A, Fig. 2) to its intersection with the liquid–vapor curve (T_h, Fig. 2). Along the isochore (between point "A" and T_h, Fig. 2), the inclusion contains a single liquid phase. With continued cooling below the homogenization temperature, the inclusion will contain both liquid and vapor, and the internal pressure in the inclusion is constrained by the pressure along the liquid–vapor curve (L + V; Fig. 2).

Most rocks in nature do not cool along a P–T path identical to the isochore for its contained fluid inclusions. As a result, the fluid inclusions generally experience internal underpressure or internal overpressure relative to the external pressure during cooling and uplift to the surface. For example, if the rock containing the fluid inclusions trapped at point A (Fig. 2) follows an isobaric path initially (path 1), followed by later isothermal uplift, the internal pressure in the inclusions would be less than the confining pressure during the entire retrograde process. Thus, at a temperature $T_{cooling}$ shown on Figure 2, the internal pressure in the inclusions would be constrained by the pressure along the isochore (P_D, as shown by point D along the isochore), whereas the confining pressure (P_B) would be determined by the intersection of the cooling path with the temperature $T_{cooling}$ (as shown by point B along the cooling path), resulting in fluid inclusions that are underpressured by an amount equal to P_B minus P_D. In this case, the fluid-inclusion cavity may decrease in size without loss of fluid, resulting in an increase in the fluid density and a concomitant decrease in the homogenization temperature. For example, if the fluid inclusion completely re-equilibrates at $T_{cooling}$ such that the inter-

nal pressure in the inclusion and the confining pressure are equal (= P_B), the re-equilibrated inclusions would homogenize at the temperature at which the new (re-equilibrated) inclusion isochore (isochore B) intersects the liquid–vapor curve, *i.e.*, $T_{h\,(B)}$ (Fig. 2). Conversely, if the rock follows an essentially isothermal path during initial stages of uplift (path 2), the confining pressure at temperature $T_{cooling}$ (Fig. 2) would be as shown by point C along the uplift path, whereas the internal pressure in the inclusion at this temperature would again be the pressure along the isochore at that temperature (point D, Fig. 2). In this case, the internal pressure in the inclusion exceeds the confining pressure by an amount equal to P_D minus P_C. Such overpressured inclusions re-equilibrate by increasing the inclusion volume, with or without loss of fluid, thus decreasing the fluid density and increasing the homogenization temperature. Thus, as depicted in example C in Figure 2, if the fluid inclusion completely re-equilibrates at $T_{cooling}$ such that the internal pressure in the inclusion and the confining pressure are equal (= P_C), the re-equilibrated inclusions would homogenize at the temperature at which the new inclusion isochore (isochore C) intersects the liquid–vapor curve, *i.e.*, $T_{h\,(C)}$ (Fig. 2).

On the basis of results of numerous studies of terrestrial samples, as well as many experimental studies

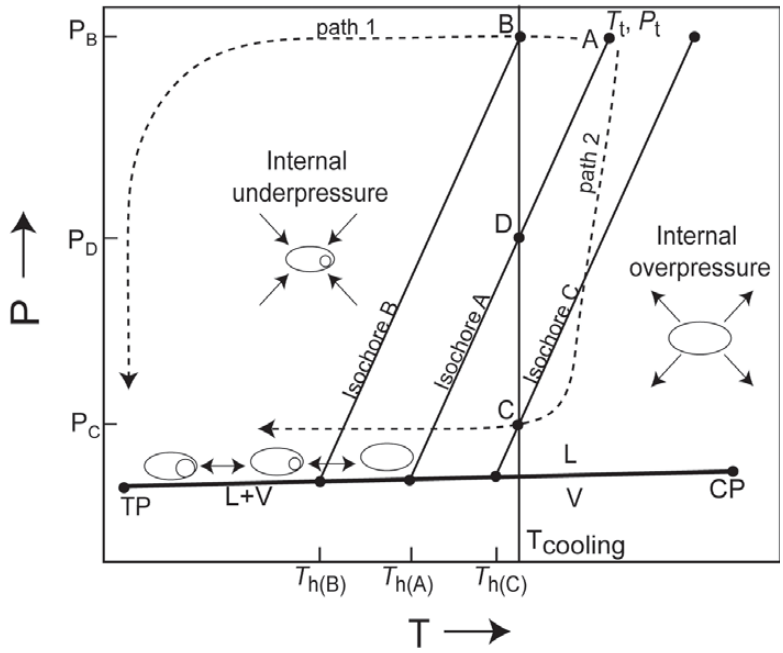

FIG. 2. Pressure–temperature conditions inside a fluid inclusion as a function of external temperature and pressure. At any temperature (T), the pressure inside a fluid inclusion containing both liquid and vapor is defined by the pressure along the liquid–vapor curve (line L + V extending from the triple point [TP] to the critical point [CP]). After the inclusion homogenizes, the pressure is defined by the pressure along the fluid isochore (line extending from the homogenization temperature [T_h] to [T_t, P_t]), trapping conditions of the inclusion. A fluid inclusion trapped at conditions T_t, P_t (point A) whose P–T cooling or uplift path corresponds to the fluid isochore (isochore A) will invariably maintain the same pressure inside of the inclusion as outside, resulting in no re-equilibration, as there is no pressure gradient. However, if the sample follows an initial isobaric cooling path (path 1), the external pressure is invariably greater than the internal pressure, and re-equilibration due to the internal underpressure may occur. The resulting decrease in the volume of the fluid inclusion produces an increase in fluid density and a decrease in homogenization temperature (*e.g.*, $T_{h\,(B)}$). If the rock follows an isothermal uplift path (path 2), the fluid inclusion may re-equilibrate owing to internal overpressures, resulting in an increase in the size of the fluid inclusion, a decrease in fluid density, and an increase in homogenization temperature (*e.g.*, $T_{h\,(C)}$). See text for details.

simulating burial or uplift (Lawler & Crawford 1983, Goldstein 1986, Sterner & Bodnar 1989, Wanamaker & Evans 1989, Bakker & Jansen 1991, Vityk *et al.* 1994, Sterner *et al.* 1995, Invernizzi *et al.* 1998, Zhang 1998, Bodnar 2003), it is well known that fluid inclusions may re-equilibrate if the P–T–t history of the sample results in a confining pressure that differs from the internal pressure in the inclusion, thereby creating a pressure gradient. Re-equilibration, as used in the fluid-inclusion literature, includes changes in volume of the fluid-inclusion cavity with no loss of fluid from the inclusion, loss of fluid from the inclusion along cracks, as well as changes in fluid density due to a combination of these processes. For a complete discussion of the different types of re-equilibration that may occur under different temperature–stress–strain conditions, the reader is referred to Bodnar (2003).

In this study, we examine the effects of impact events and the resultant shock-wave on the extent of survival and homogenization temperature of fluid inclusions. The homogenization temperatures of aqueous fluid inclusions in quartz were measured before and after being subjected to experimentally simulated shock-waves of known magnitude in order to determine if the inclusion volume increased, decreased, or remained unchanged as a result of the impact. Quartz was chosen as the host mineral in this study because it has been the most thoroughly investigated mineral in studies of fluid-inclusion re-equilibration. Similarly, the shock behavior of quartz is well characterized, and quartz serves as the standard to delineate the shock history of common terrestrial rocks (Stoffler & Langenhorst 1994). These background studies identify quartz as the ideal starting material to evaluate the general behavior of fluid inclusions under shock, yet we realize that quartz is not found in meteorites. Moreover, the effects of non-isochoric confining conditions on fluid inclusions in minerals commonly found in meteorites (*e.g.*, olivine, pyroxene, carbonates, sulfates, halides) are not well documented, making application of the results from this study to meteorites difficult. Experimental investigations similar to those discussed here but on minerals more commonly found in meteorites are necessary to fully understand the effects of shock metamorphism on fluid inclusions in meteorites. This study merely provides a starting point for an observation and a quantification of the effects of shock metamorphism on the properties of fluid inclusions.

Pressure–Temperature Conditions During Impact

Impact events result in shock deformation due to the extremely high strain-rates and pressures created by the shock wave originating at the point of impact, as well as the elevated temperatures resulting from the entropy gain of the impacted material. Using the experimentally determined equation of state (EOS) of quartz from Wackerle (1962), Gratz *et al*. (1992) calculated the shock pressures and temperatures of quartz during small-scale impacts similar to the experimental conditions of this study. Their P–T–t data (Fig. 3) indicate that maximum conditions of shock pressure and temperature are reached within 1–2 microseconds using flat metal plates of millimeter thickness simulating the projectile. The duration for the target rock to reside at elevated pressures is linearly related to the dimensions of the projectile and is on the order of μs in experimental impacts, but can approach seconds in basin-scale, natural events. Waste heat is generated upon adiabatic decompression of the sample to ambient pressures. This thermal energy takes a relatively long time to dissipate, and the sample remains at elevated temperatures for a considerable period of time, compared to the amount of time the sample experiences elevated pressures.

Fluid inclusions that follow the P–T path predicted by Gratz *et al.* (1992) experience an initial internal underpressure in the fluid inclusions, as the amplitude of the shock wave far exceeds the isochoric pressure within the inclusion (Fig. 4). This is followed by a period of internal overpressure during extended heating of the sample at ambient pressure; the isochoric pressure within the inclusion remains high as a result of the elevated temperatures. For example, less than one μs after impact, the P–T conditions of the sample would reach 500 K and approximately 5 GPa (point "A", Fig. 4). At this same time, the internal pressure in a fluid inclusion with a homogenization temperature of 373 K (100°C) would be about 0.2 GPa (point "B", Fig. 4), resulting in an internal underpressure of about 4.8 GPa.

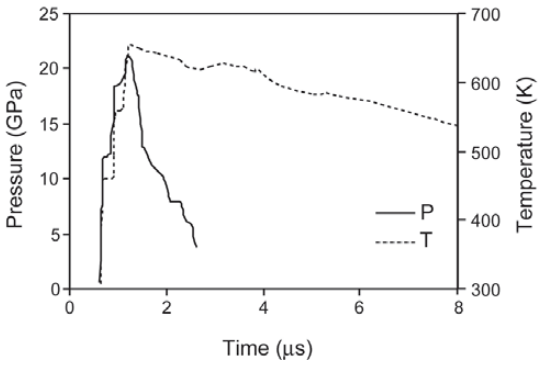

FIG. 3. Pressure – temperature – time evolution of quartz resulting from a 22 GPa shock event, based on hydrodynamic modeling of Gratz *et al.* (1992), using experimental conditions similar to those employed in the present study. Within the first 2 μs after impact, pressure and temperature have reached their maximum values. After 3 μs, the pressure has returned to pre-shock conditions. The temperature, however, remains high for an extended period as the sample slowly cools.

After about 4 μs, the shock pressure will have decreased to ambient pressure (0.0001 GPa), but the temperature of the sample has only cooled to 500 K (point "C", Fig. 4). Owing to the elevated temperature, the internal pressure in the inclusion will be about 0.2 GPa at this time (point "B", Fig. 4), whereas the confining pressure is only 0.0001 GPa, resulting in an internal overpressure of about 0.2 GPa. A fluid inclusion subjected to the P–T–t history shown in Figures 3 and 4 would thus initially undergo compression, resulting in an increased density of the fluid and a lower temperature of homogenization (Sterner & Bodnar 1989, Vityk & Bodnar 1995). This initial re-equilibration would then be overprinted by stretching of the fluid inclusions, resulting in a decreased density of the trapped fluid and a higher temperature of homogenization (Bodnar *et al.* 1989, Bodnar 2003). Extreme compression of fluid inclusions could result in the complete collapse of the inclusion vesicle (see Vityk & Bodnar 1995, their Fig. 6H), whereas expansion of the inclusion could lead to decrepitation with complete loss of fluid along microcracks or dislocations to produce empty voids.

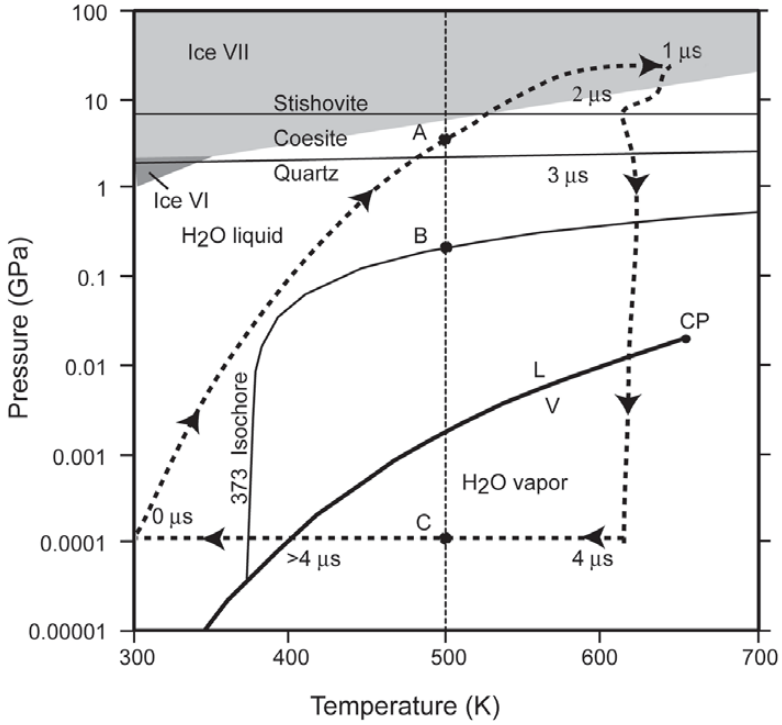

FIG. 4. Pressure – temperature – time path of quartz during a 22 GPa impact event. The dashed line with arrows approximates the P–T–t path of the sample [using data from Gratz *et al.* (1992), shown in Fig. 3]. The thin line labeled "373 isochore" represents the isochore for a fluid inclusion that homogenizes at 373 K (100°C). Stability fields for various phases of H2O are also shown: the light gray field at high pressure shows the stability field of ice VII, the small dark gray wedge at moderate pressure and low temperature represents the stability field of ice VI. The bold line (labeled L/V) that ends at the critical point (CP) of water is the liquid–vapor curve for H_2O. Phase boundaries for the SiO_2 polymorphs stishovite, coesite and quartz are shown as thin, nearly horizontal lines at elevated pressure. Where the P–T path is above the fluid isochore (such as at point "A"), the fluid inclusions are underpressured, and where the P–T path is below the fluid isochore (such as at point "C"), the inclusions are overpressured. Note that immediately following impact, the fluid inclusions experience a significant internal underpressure. The quartz host also passes through the coesite field and into the stability field of stishovite during this event. After the high-pressure shock wave has traveled through the sample and the pressure returns to ambient conditions, the temperature of the sample remains high for an extended period as the quartz slowly cools, resulting in an extended period of internal overpressure within the fluid inclusions.

At low to moderate shock pressures (≤9–15 GPa), below the Hugoniot Elastic Limit of quartz (HEL: the transition from brittle to plastic deformation; Wackerle 1962), the impact is accommodated by brittle deformation of the shocked quartz, potentially leading to leakage of fluid inclusions along microcracks. At shock conditions above the Hugoniot Elastic Limit, materials behave plastically, and the original structure of the crystal gets deformed (Poirier 1991), potentially destroying fluid inclusions owing to the movement of fluids along dislocations (Bakker & Jansen 1990, Vityk *et al*. 2000). Likewise, recrystallization of the host mineral due to reconstructive phase-transitions or formation of amorphous material at still higher shock pressures may also erase any record of fluid inclusions, as H_2O may be lost from the system (or accommodated structurally into new phases, although this is not known for quartz).

Methods

Disks (7.3 mm diameter, 1 mm thick) were cut from single, centimeter-size Arkansas quartz crystals (Engle 1952), polished, examined petrographically, and photographed. Each disk contained several planes or trails of fluid inclusions of varying size and shape, but with similar liquid:vapor ratios and, presumably, similar temperatures of homogenization. No one-phase inclusions, inclusions with daughter crystals, or inclusions containing more than two fluid phases were observed.

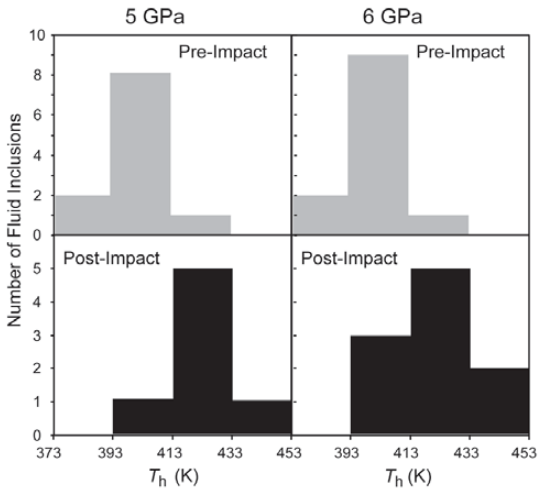

FIG. 5. Comparison of pre- and post-impact temperatures of homogenization (T_h). Pre-impact T_h data are nearly identical for both samples, ranging from 373 to 433 K, with the mode between 393 and 413 K. The post-impact range in T_h is shifted to temperatures 20 K higher, as is the mode in both the 5 and 6 GPa experiments, indicating re-equilibration due to internal overpressures.

Ideally, we would have measured the homogenization temperature of every fluid inclusion in every quartz disk to be used in the impact experiments. However, given the large number of disks and the large number of inclusions in each disk (several hundred), measuring the homogenization temperature of every inclusion was not practical. Therefore, a plan was developed that would allow us to characterize the mode as well as the complete range (minimum and maximum) of homogenization temperatures in each disk. To accomplish this, a few inclusions from each plane or trail in the disk were selected and monitored during heating. Each disk was heated slowly from room temperature in a USGS-type heating stage (Roedder 1984) to first determine the minimum temperature of homogenization of the entire suite of fluid inclusions in the disk (*i.e.*, no inclusions homogenized below this temperature). Once this minimum temperature was determined, the disk was then heated in small increments (either 5, 10 or 20 K), held at temperature, and monitored to determine which, if any, of the pre-selected inclusions had homogenized during the heating increment. This procedure was continued until all of the pre-selected inclusions had homogenized. Then the sample was scanned to determine if any other unhomogenized inclusions still remained. If so, stepped heating was continued until every observable inclusion in the sample had homogenized; this then defined the maximum temperature of homogenization for the complete suite of inclusions in the sample.

Pre-impact temperatures of fluid-inclusion homogenization were very uniform from one disk to the next, and ranged from 373 to 433 K, with the mode lying between 393 and 413 K (Fig. 5). The approach used here

TABLE 1. SUMMARY OF EXPERIMENTAL CONDITIONS AND OBSERVATIONS

Target number	Velocity km/s	Projectile material*	Projectile mass g	Shock pressure GPa	Fluid-inclusion characteristics
16	1.21	Poly Lexan	9.09	5.0	FIs present T_h increase ~ 20 K
1	1.39	Poly Lexan	9.08	6.0	FIs present T_h increase ~20 K Decrepitated FIs Collapsed FIs
6	0.97	Poly Al2024	9.80	7.6	Decrepitated FIs Collapsed FIs
18	1.04	Poly Al2024	9.76	8.4	Collapsed FIs
7	1.20	Poly Al2024	9.73	10.0	Collapsed FIs
3	1.43	Poly Al2024	9.64	12.4	Collapsed FIs ?
4	1.41	Poly Al2024	9.71	18.0	No FI textures
5	1.13	Poly SS304	12.32	24.2	No FI textures
2	1.39	Poly SS304	12.80	30.8	No FI textures

* The first half of the entry (in all experiments "Poly") refers to the polyethelene body of the projectile. The second half refers to the flat plate at the head of the projectile that collides with the sample.

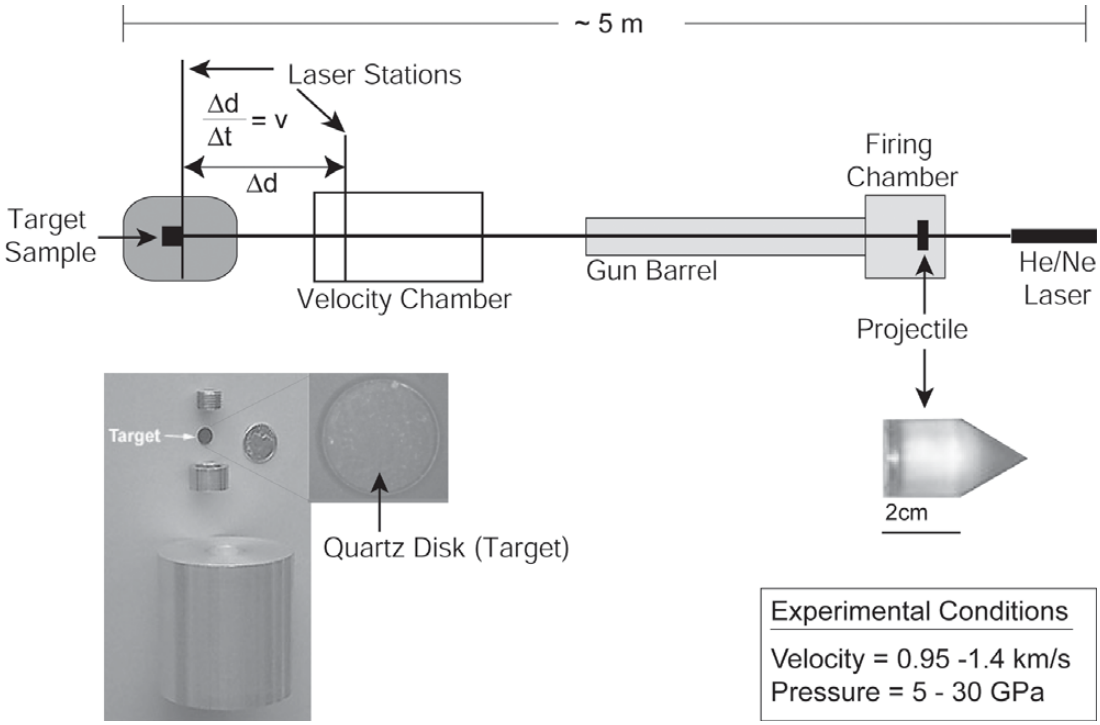

FIG. 6. Schematic representation of NASA's Experimental Impact Laboratory Flat Plate Accelerator (http://ares.jsc.nasa.gov/education/websites/craters/gunlabtour.htm). See text for experiment description. The diagram is not to scale; total length of Flat Plate Accelerator is ~5 m.

to characterize the complete range of pre-impact temperatures of homogenization was viable only because of the homogeneity of fluid inclusions within the sample, with all inclusions homogenizing over a small range in temperature. If each sample had shown a wide range in homogenization temperatures, this approach would not have been valid.

The quartz disks were subjected to planar shock waves of known amplitude using a powder-propellant gun 25 mm in caliber to accelerate flat metal flyer-plates (Table 1, Fig. 6). Experimental details are given in Skala *et al.* (2002). The sample disk was inserted into a jacket of Aluminum Alloy 2024 (Al2024) or Stainless Steel 304 (SS304) and placed at a distance of 0.5 mm from the machined surface to be impacted by flat flyer-plates. The latter were some 20 mm in diameter and 2 mm thick, composed of either Lexan, Al2024, or SS304. These flyer-plates form the flat face of a cylindrical polyethylene projectile. Approximate speed of the projectile is predicted from the measured weight ratio of the propellant powder and projectile, yet it is measured to better than 1% *via* occultation of multiple lasers (four stations) trained onto photodiodes. The equations of state of all materials used for the metal jackets and flyer plates are known (*e.g.*, Marsh 1980); it suffices then to measure impact speed only and to apply a graphical impedance-match method to obtain the peak pressure experienced by the quartz sample, following multiple reverberations of the shockwave (Duval 1962). For further details, the reader is referred to NASA's Experimental Impact Laboratory website (http://ares.jsc.nasa.gov/education/websites/craters/gunlabtour.htm).

The shocked disks were machined from the metal sample holder using liquid nitrogen as a coolant, impregnated with epoxy, repolished, and examined petrographically. If fluid inclusions were found within the shocked samples, their homogenization temperatures were again measured in 20 K steps on the USGS heating stage.

The shocked disks were also analyzed using Raman spectroscopy to search for evidence of any high-pressure phases or diaplectic glass in the samples. The spectra were compared to spectra for an unshocked sample of Arkansas quartz. The Raman analyses were obtained on a JY Horiba LabRam 300 mm instrument using a 532.09 nm excitation wavelength and 100× objective, with the sample oriented parallel to the *c* axis. Accumulation times (5 s for the unshocked sample, 10 s for the

18 GPa, and 60 s for the 24 and 30 GPa samples) varied among the samples in order to maintain an approximately constant intensity for the major peak at about 465 cm^{-1}. For each sample, five spectra were collected on the same spot and averaged to give the final spectrum.

Results

The petrographic features of fluid inclusions in the shocked samples belong to one of four categories: (1) relatively *pristine* fluid inclusions, (2) *decrepitated* (or leaked) fluid inclusions, (3) *collapsed* fluid inclusions, and (4) *no optical evidence* of fluid inclusions remaining (Fig. 7). Relatively pristine fluid inclusions were observed only in samples shocked at the lowest pressure, 5 and 6 GPa. Decrepitated fluid inclusions have no recognizable vapor bubble and were found in samples shocked at 6 and 7.6 GPa. Textures similar to those observed in samples experimentally re-equilibrated at conditions of internal underpressures (Vityk & Bodnar 1995) were observed in samples shocked at 7.6, 8.4, and 10 GPa, and are interpreted as collapsed fluid inclusions. The disk shocked at 12 GPa contained two very small features similar to these collapse textures; however, no further evidence of fluid-inclusion features was observed in the sample. Samples shocked at 18 GPa and higher contained no evidence of fluid inclusions following the impact experiment.

The samples shocked at 5 and 6 GPa show a significant decrease in the number of fluid inclusions present. Fluid inclusions were found in both heavily fractured areas and those areas in which the quartz remained relatively clear. The highest concentration of preserved fluid inclusions was found in a clear area of the 6 GPa sample, separated from the rest of the disk by fractures, which appeared to be mainly unaffected by shock deformation. The inclusions observed within the 5 and 6 GPa shocked samples could not be matched with the pre-impact fluid inclusions documented in the disks, so no direct comparison of homogenization temperatures can be made. However, the range of homogenization temperatures (393–453 K) and the mode (413–433 K) observed in both the 5 and 6 GPa post-shock samples show a distinct increase compared to pre-impact results (Fig. 5), suggesting that the inclusions have expanded during the

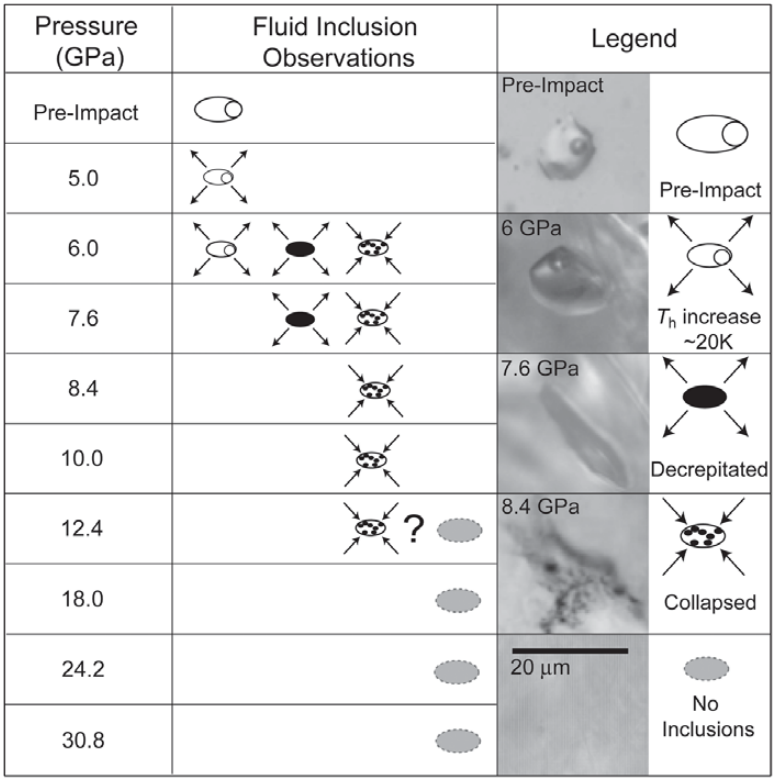

FIG. 7. Evolution of features of fluid inclusions with increasing shock pressure. The bar scale shown applies to all five photomicrographs. See text for details.

impact event (or have lost some fluid), resulting in a lower bulk-density of the fluid. Decrepitated (or leaked) fluid inclusions were also observed in the 6 GPa sample. Both the increase in homogenization temperatures and the presence of decrepitated fluid inclusions are likely the result of internal overpressures accompanying the elevated temperatures following the impact event. No evidence for re-equilibration during the short period of internal underpressure that occurred during the first few microseconds following impact was found in the 5 and 6 GPa samples. Any such features have likely been overprinted by the longer, high-temperature overpressure conditions that followed.

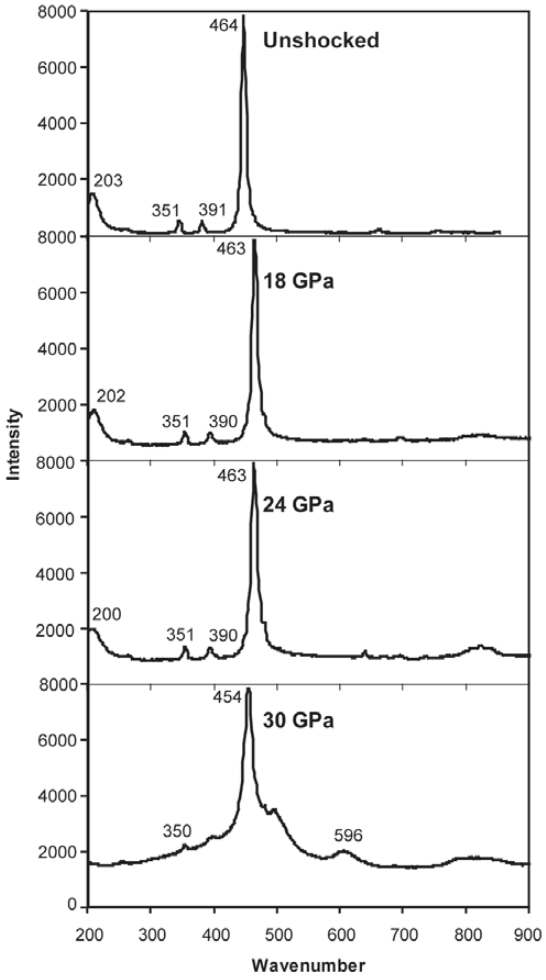

FIG. 8. Raman spectra of quartz samples (intensity normalized). Unshocked sample of quartz shows a narrow main peak at 464.8 cm^{-1}. The 18 GPa sample produces a similar spectrum with no discernible shift or broadening of the 464 cm^{-1} peak. At 24 GPa, the main peak of quartz has shifted to slightly lower wavenumber and begins to show signs of broadening, indicative of a diaplectic glass component. In the 30 GPa sample, the main peak of quartz is broader and shifted to 455 cm^{-1}.

No intact fluid inclusions were found within samples shocked at pressures ≥7.6 GPa. Very few decrepitated inclusions were found in the 6.0 and 7.6 GPa samples. However, groupings of small dark features were observed in the 6.0, 7.6, 8.4, and 10 GPa samples. These groupings of what may be very small (≤1 μm) inclusions contained within an area of anomalously textured quartz are similar to inclusions experimentally subjected to conditions of high external overpressure, effectively collapsing the fluid inclusions (Vityk & Bodnar 1995; their Fig. 6H). These "collapse" features would thus seem to have formed during the compressive phase of the shock event. Two small features similar to these collapse features were also observed in the 12 GPa sample. No other evidence of the former presence of fluid inclusions was found in this sample, however.

No optical evidence for the survival of fluid inclusions was found in samples subjected to shock pressures greater than 12 GPa. The samples are nearly opaque, with the amount of petrographically recognizable quartz decreasing with increasing shock pressure. Above 9–15 GPa (the Hugoniot elastic limit), quartz no longer deforms elastically during impact. Instead, the crystal structure begins to deform plastically, and the crystal structure of quartz is severely disrupted (Horz & Quaide 1972). At still higher pressures, shock-induced conversion to an isotropic material begins, and any fluid inclusions as well as the crystal structure will be destroyed.

Raman analysis of the shocked samples showed no evidence of coesite or stishovite in any of the disks. However, in the 30 GPa sample, the main peak of quartz (observed in unshocked quartz at 464 cm^{-1}) is broadened and shifted to lower wavenumbers (Fig. 8), indicating that the sample contains a mixture of diaplectic glass and quartz (McMillan *et al*. 1992). The 24 GPa sample also appears to contain a small component of the amorphous phase, whereas the spectrum from the 18 GPa disk matches that of unshocked quartz.

CONCLUSIONS

This experimental study of shock metamorphism demonstrates that fluid inclusions undergo a systematic and gradual evolution in re-equilibration effects with increasing shock pressures. Fluid inclusions in single-crystal quartz can survive low levels of shock metamorphism, up to 6 GPa. The homogenization temperatures of fluid inclusions in these modestly shocked samples increased an average of ~20 K compared to pre-impact homogenization temperatures, suggesting re-equilibration due to internal overpressure. This increase most likely results from extended heating of the samples following impact. In all cases, those inclusions that are preserved show increased temperatures of homogenization, compared to pre-shock samples. Therefore, ho-

mogenization temperatures measured for fluid inclusions in meteorites and terrestrial impactites should be considered a maximum value, as the density of the original trapped fluid was likely greater than that observed in the inclusions following the impact event.

Only decrepitated or collapsed fluid inclusions were observed in samples experiencing 7–10 GPa shocks. The collapse features observed in these samples are similar to experimentally produced collapsed fluid inclusions. However, it remains unclear if these textures may also form because of internal overpressure conditions. No optical evidence of fluid inclusions was found in quartz shocked at pressures greater than 12 GPa. Plastic deformation of the host mineral may have completely destroyed the petrographic features of pre-impact fluid inclusions.

This systematic progression of shock-induced re-equilibration features may be used to estimate syn- and post-impact pressure–temperature conditions experienced by quartz-bearing rocks, especially at pressures lower than 10 GPa that seem otherwise difficult to resolve optically (*e.g.*, Stoffler & Langenhorst 1994). The experimental results may also apply to feldspars, which do occur in meteorites. Feldspars display shock behavior that is qualitatively similar to quartz (*e.g.,* Ostertag 1983). Other phases reported from meteorites to contain fluid inclusions (carbonates, sulfates, halides) are more compressible than tectosilicates like quartz and feldspar-group minerals, suggesting that their fluid inclusions may be greatly affected at still lower shock stresses, whereas those in olivine may be modestly more resistant. Our results thus indicate that the absence of fluid inclusions in meteoritic materials does not preclude the presence of fluids on meteorite parent bodies. Instead, all previously trapped fluid inclusions may have been destroyed by relatively modest shock processes.

Acknowledgements

The authors thank Craig Altare for help with sample preparation and Charles Farley for assistance with Raman measurements. Reviews by John Spray and an anonymous reviewer were helpful in clarifying and improving the manuscript.

References

Bakker, R. & Jansen, J.B.H. (1991): Experimental post-entrapment water loss from synthetic CO_2 – H_2O inclusions in natural quartz. *Geochim. Cosmochim. Acta* **55**, 2215-2230.

Bischoff, A. (1998): Aqueous alteration of carbonaceous chondrites: evidence for preaccretionary alteration: a review. *Meteor. Planet. Sci.* **33**, 1114-1122.

Bodnar, R.J. (1999): Fluid inclusions in Allan Hills 84001 and other martian meteorites: evidence for volatiles on Mars. *Lunar Planet. Sci. Inst. XXX, Abstr.* 1222 (CD-ROM).

_____ (2002): Re-equilibration of fluid inclusions. *In* Fluid Inclusions: Analysis and Interpretation (I. Samson, A. Anderson & D. Marshall, eds.). *Mineral. Assoc. Canada, Short Course Vol.* **32**, 213-231.

_____, Binns, P. & Hall, D.L. (1989): Synthetic fluid inclusions. VI. Quantitative evaluation of the decrepitation behavior of fluid inclusions in quartz at one atmosphere confining pressure. *J. Metamorph. Geol*. **7**, 229-242.

Bridges, J., Catling, D., Saxon, J., Swindle, T., Lyon, I. & Grady, M. (2001): Alteration assemblages in Martian meteorites: implications for near-surface processes. *Space Science Rev.* **96**, 365-392.

Bridges, J. & Grady, M. (2000): Evaporite mineral assemblages in the nakhlite (martian) meteorites. *Earth Planet. Sci. Lett.* **176**, 267-279.

Duval, G.E. (1962): Concepts of shock wave propagation. *Bull. Seismol. Soc. Am.* **52**, 869-893.

El Goresy, A., Dubrovinsky, L., Sharp, T.G., Saxena, S.K. & Chen, Ming (2000): A monoclinic post-stishovite polymorph of silica in the Shergotty meteorite. *Science* **288**, 1632-1634.

Engel, A.E.J. (1952): Quartz crystal deposits of western Arkansas. *U.S. Geol. Surv., Bull.* **973-E**, 173-260.

Fritz, J, Greshake, A. & Stoffler, D. (2003): Launch conditions for Martian meteorites: plagioclase as a shock pressure barometer. *Lunar Planet. Sci. Center XXXIV, Abstr.* **1335** (CD-ROM).

Goldstein, R. (1986): Re-equilibration of fluid inclusions in low-temperature calcium-carbonate cement. *Geology* **14**, 792-795.

Gratz, A.J., Nellis, W.J., Christie, J.M., Brocious, W., Swegle, J. & Cordier, P. (1992): Shock metamorphism of quartz with initial temperatures –170 to +1000°C. *Phys. Chem. Minerals* **19**, 267-288.

Greshake, A. (1998): Transmission elecron microscopy characterization of shock defects in minerals from Nakhla SNC meteorite. *Meteor. Planet. Sci.* **33**(suppl.), A63 (abstr.).

Horz, F. & Quaide, W. L. (1972): Debye–Scherrer investigations of experimentally shocked silicates. *The Moon* **6**, 45-82.

Invernizzi, C., Vityk, M., Cello, G. & Bodnar, R. (1998): Fluid inclusions in high pressure/low temperature rocks from the Calabrian Arc (southern Italy): the burial and exhumation history of the subduction related Diamante–Terranova unit. *J. Metamorph. Geol.* **16**, 247-258.

Koeberl, C., Fredriksson, K., Gotzinger, M. & Reimold, W.U.U. (1989): Anomalous quartz from the Roter Kamm impact crater, Namibia: evidence for post-impact hydrothermal activity? *Geochim. Cosmochim. Acta* **53**, 2113-2118.

KOMOR, S., VALLEY, J.W. & BROWN, P.E. (1988): Fluid-inclusion evidence for impact heating at the Siljan Ring, Sweden. *Geology* **16**, 711-715.

LANGENHORST, F. (1994): Shock experiments on pre-heated α and β quartz. II. X-ray and TEM investigations. *Earth Planet. Sci. Lett.* **128**, 683-698.

_____ & GRESHAKE, A. (1999): A transmission electron microscope study of Chassigny: evidence for strong shock metamorphism. *Meteor. Planet. Sci.* **34**, 43-48.

LAWLER, J.P. & CRAWFORD, M.L. (1983): Stretching of fluid inclusions resulting from a low-temperature microthermometric technique. *Econ. Geol.* **78**, 527-529.

MALAVERGNE, V., GUYOT, F., BENZERARA, K. & MARTINEZ, I. (2001): Description of new shock-induced phases in the Shergotty, Zagami, Nakhla, and Chassigny meteorites. *Meteor. Planet. Sci.* **36**, 1297-1305.

MARSH, S.P. (1980): *LASL Shock Hugoniot Data*. University of California Press, Berkeley, California.

MCMILLAN, P.F., WOLF, G.H. & LAMBERT, P. (1992): A Raman spectroscopic study of shocked single crystalline quartz. *Phys. Chem. Minerals* **19**, 71-79.

OSTERTAG, R. (1983): Shock experiments on feldspar crystals. *Proc. Lunar Planet. Sci. Conf. 14th, J. Geophys. Res.* **88**, B364-B376.

POIRIER, J. (1991): *Introduction to the Physics of the Earth's Interior*. Cambridge University Press, Cambridge, U.K.

ROEDDER, E. (1984): Fluid Inclusions. *Rev. Mineral.* **12**.

RUBIN, A.E., SCOTT, E.R.D. & KEIL, K. (1997): Shock metamorphism of enstatite chondrites. *Geochim. Cosmochim. Acta* **61**, 847-858.

_____, ZOLENSKY, M.E. & BODNAR, R.J. (2002): The halite-bearing Zag and Monahans (1998) meteorite breccias: shock metamorphism, thermal metamorphism and aqueous alteration on the H-chondrite parent body. *Meteor. Planet. Sci.* **37**, 125-141.

SCHMITT, R. & STOFFLER, D. (1995): Experimental data in support of the 1991 shock classification of chondrites. *Meteoritics* **30**, 574-575.

SKALA, R., EDEROVA, J., MATEJKA, P. & HORZ, F. (2002): Mineralogical investigations of experimentally shocked dolomite: implications for the outgassing of carbonates. *Geol. Soc. Am., Spec. Pap.* **356**, 571-585.

STERNER, S.M. & BODNAR, R.J. (1989): Synthetic fluid inclusions. VII. Re-equilibration of fluid inclusions in quartz during laboratory-simulated metamorphic burial and uplift. *J. Metamorph. Geol.* **7**, 243-260.

_____, HALL, D.L. & KEPPLER, H. (1995): Compositional re-equilibration of fluid inclusions in quartz. *Contrib. Mineral. Petrol.* **119**, 1-15.

STOFFLER, D., KEIL, K.& SCOTT, E.R.D. (1991): Shock classification of ordinary chondrites. *Geochim. Cosmochim. Acta* **55**, 3845-3867.

_____ & LANGENHORST, F. (1994), Shock metamorphism of quartz in nature and experiment. I. Basic observation and theory. *Meteoritics* **29**, 155-181.

_____, OSTERTAG, R., JAMMES, C., PFANNSCHMIDT, G., SEN GUPTA, P.R., SIMON, S.B., PAPIKE, J.J. & BEAUCHAMP, R.H. (1986): Shock metamorphism and petrology of the Shergotty achondrite. *Geochim. Cosmochim. Acta* **50**, 889-903.

TUGARINOV, A.I. & NAUMOV, V.B. (1970): Dependence of the decrepitation temperature of minerals on the composition of their gas–liquid inclusions and hardness. *Dokl. Akad. Nauk SSSR* **195**, 112-114 (in Russ.).

ULRICH, M.R. & BODNAR, R.J. (1988): Systematics of stretching of fluid inclusions. II. Barite at one atmosphere confining pressure. *Econ. Geol.* **83**, 1037-1046.

VITYK, M.O. & BODNAR, R.J. (1995): Textural evolution of synthetic fluid inclusions in quartz during re-equilibration, with application to tectonic reconstruction. *Contrib. Mineral. Petrol.* **121**, 309-323.

_____, _____ & DOUKHAN, J.-C. (2000): Synthetic fluid inclusions. XV. TEM investigation of plastic flow associated with re-equilibration of synthetic fluid inclusions in natural quartz. *Contrib. Mineral. Petrol.* **139**, 285-297.

_____, _____ & SCHMIDT, C.S. (1994): Fluid inclusions as tectonothermobarometers: relation between pressure–temperature history and re-equilibration morphology during crustal thickening. *Geology* **22**, 731-734.

WACKERLE, J. (1962): Shock-compression of quartz. *J. Appl. Phys.* **33**, 922-937.

WANAMAKER, B.J. & EVANS, B. (1989): Mechanical re-equilibration of fluid inclusions in San Carlos olivine by power-law creep. *Contrib. Mineral. Petrol.* **102**, 102-111.

ZHANG, YOUXUE (1998): Mechanical and phase equilibria in inclusion–host systems. *Earth Planet. Sci. Lett.* **157**, 209-222.

ZOLENSKY, M.F., BODNAR, R.J., GIBSON, E.K., JR., NYQUIST, L.E., REESE, Y., SHIH, CHI-YU & WIESMANN, H. (1999): Asteroidal water within fluid inclusion-bearing halite in an H5 chondrite Monahans (1998). *Science* **285**, 1377-1379.

_____ & MCSWEEN, H.Y., JR. (1988): Aqueous alteration. *In* Meteorites and the Early Solar System (J.F. Kerridge & M.S. Mathews, eds.). University of Arizona Press, Tucson, Arizona (114-143).

Received January 25, 2003, revised manuscript accepted March 12, 2004.